

Kinematics, Dynamics and Control of Wheeled Mobile Robots

Yilin Zhao and Spencer L. BeMent

Department of Electrical Engineering and Computer Science
The University of Michigan
Ann Arbor, MI 48109

Abstract

The controllability of nonholonomic robot systems is proved for six common wheel and axle configurations that possess two or three degrees of freedom. After the kinematics and dynamics were modeled using the synchro-drive vehicle as an example, we prove that continuous feedback stabilization of the vehicle to an equilibrium point is impossible. The dynamic model so developed are also used to prove that simple controllers are sufficient to guarantee stability for the drive- and steering-angle components of synchro-drive vehicles. Although the underlying control systems are stable, the experimental results demonstrated that potential-field navigation can lead robot trajectories to an unexpected invariant set. The results reported here can easily be extended to the modeling and control of other mobile robot systems.

1 Introduction

Interest in mobile robots is growing rapidly because of the very broad range of their potential applications. The challenge is that these robots move intelligently so that they can perform various actions without human intervention. In contrast with robot manipulators, mobile-robot systems are nonholonomic systems because their constraint equations are not integrable [8]. This makes the analysis of their kinematics, dynamics, and control more complex because coordinates cannot be eliminated by using the equations of constraint. Systems with nonholonomic constraints therefore always require a larger number of coordinates for their description than their number of degrees of freedom. In general, based on the dimension of the movement, a mobile robot can be classified into one of three categories: 1) it follows a fixed and constrained straight-line path, such as inside pipes or channels; 2) it moves on a plane, such as the floor of a building; or 3) it maneuvers in space or under water.

Research groups and commercial companies world wide have built many different mobile robots that move on a plane. Although these robots have different wheel and axle configurations, in general they can be divided into two groups, either 2-degrees-of-freedom (2-DOF) or 3-degrees-of-freedom (3-DOF) robots. In dynamics, the number of degrees of freedom is defined as the number of coordinates used to specify the configuration of the system minus the number of independent equations of constraint [8]. For instance, a 2-DOF mobile robot could be a three-wheel vehicle with two drive wheels and one caster wheel and a 3-DOF mobile robot could be a three-wheel vehicle with two drive wheels and one steering wheel or four omni-directional wheels, etc.

Many researchers have developed methodologies for the kinematic and dynamic modeling of wheeled mobile robots. An ex-

tensive study of this subject was published by Muir [13]. A three-wheeled 2-DOF mobile robot was modeled by Saha and Angels [15]. Alexander and Maddocks [1] studied the planar rigid-body motions which can be achieved for a given wheel configuration and the steering and drive rates that access the motions. A particular case of three-wheeled robot (two-front wheel and one-rear wheel) was recently modeled by d'Andréa-Novel, Bastin and Campion [6]. However, we have found no mention in the literature of any modeling of the widely used Cybermation [9] and Denning [16] robots, although the special features of their synchronous drive and steering mechanism tend to facilitate analysis and control. The unique synchronization characteristic of these systems is that their three wheels are locked together by a set of belts, chains or concentric shafts with bevel gears. One motor is used to drive and another to steer the wheels. The steering belts, chains or bevel gears are connected to a spine shaft that runs vertically through the center of the platform. Thus a payload mounted on the top of the shaft rotates with the wheels while the main body of the platform maintains its orientation to the world coordinate system with minimal precession.

It is important to study the kinematics, dynamics, and control of these popular synchro-drive vehicles. Since no model is available for synchro-drive vehicles, it is difficult to analyze the dynamic behavior of these systems. Users issue commands to such vehicles manually or via software based on the assumption that the vehicle will take a predictable course of action, which is not always true. A theoretical framework will provide a better understanding of the response of these systems. Moreover, good models for such systems can also provide a basis for synchro-drive vehicle simulation. In short, an in-depth analysis should aid significantly in the design, simulation, and control of synchro-drive vehicles as well as for other mobile robots.

Impressive progress is being made in the mobile-robot field, as evidenced by the growing volume of research papers published each year. Quite recently, nonlinear control theory was introduced into this field [12]. This led to the study of navigating mobile robots using nonlinear feedback control rather than algorithmic or heuristic motion planning. By briefly analyzing traditional control methods mathematically, we illustrate the difficulties associated with analytical studies of other methods. In the next section we summarize the basic requirements for a mobile robot system to use nonlinear-feedback control techniques for navigation. Since a frequently used example in this study is a front-wheel-drive car-like robot [3, 11], we try here to cover the most commonly used mobile robots and their related controllability problems. This study should provide adequate foundation for people interested in using nonlinear-control or related methods for motion planning.

Using the synchro-drive vehicle as an example, we then ana-

lyze the modeling and control of mobile robots. From this analysis, kinematic equations are derived for the simulation used in [18]. Dynamic equations are also derived. Using an equivalent transformation to the kinematic equations, we prove that a continuous feedback-control law does not exist for the smooth stabilization to an equilibrium point. Using the dynamic equations, we show that a simple controller can stabilize the vehicle system at a desired given angular position. From this and from nonlinear control studies, we know that these traditional control techniques have a solid mathematical foundation and can be studied analytically, although some problems may require a strong mathematical background. In contrast, the nontraditional techniques are very difficult to analyze. For instance, although the underlying position-control systems of synchro-drive vehicles are stable, as shown in [19], one popular control algorithm, the potential-field method, can suffer from the local minimum problem, as evidenced in an experimental study discussed in 5.2.3. In short, this algorithm could lead robot trajectories to an invariant set and associated limit-cycle performance. We believe that this paper is the first to point out that an invariant set exists under potential-field control. In other words, the theoretical analysis of the potential field and its related methods is very difficult. We hope that the present study will promote further interest in this area.

2 Controllability of Wheeled Mobile Robots

The controllability of wheeled mobile robots is very important for the analysis of underlying trajectory-tracking control systems. Without an adequate understanding of these control systems and in the absence of a reliable tracking system, high level planning cannot easily be performed successfully. In recent years significant progress has been made in the application of differential geometric methods to nonlinear control systems [10, 14]. We use here part of differential geometric theory which is directly applicable to mobile robot control problems. These problems have proved to be difficult to solve by other methods.

Since we are interested in describing the mobile robot with respect to the world coordinate system, the kinematic equations of the mobile robot are given as follows:

$$\dot{p} = J(p)\dot{q}, \quad (1)$$

where $p \in R^n$ is a generalized coordinate vector, $\dot{q} \in R^m$ is an input vector to the system, and $n > m$. Rewriting the above equation to the conventional form for nonlinear control, we get

$$\dot{p} = f(p) + \sum_{i=1}^m g_i(p)u_i, \quad (2)$$

where $p \in R^n$, $u = [u_1, u_2, \dots, u_m]^t = \dot{q}$, t denotes a transpose, and f and g_i are real analytic vector fields on R^n . For the mobile robot system, $n - m$ nonholonomic constraints are written in the form

$$\sum_{i=1}^n a_{ji}\dot{p}_i + a_j = 0; \quad (j = 1, 2, \dots, m) \quad (3)$$

where the a_{ji} is in general a function of p and time and a_j equals zero.

Theorem 1 *Given a wheeled mobile-robot system (2), the system is locally accessible¹ around a point $p_c \in R^n$ if it satisfies*

¹Some researchers use weakly controllable [10] instead of locally accessible.

the accessibility rank condition at p_c , that is, its accessibility distribution spans R^n at the point p_c .

Proofs for Theorems 1, 2 and 4 and the six corollaries that follow can be found in [19], Chapter II, along with related definitions. The proof of Theorem 3 is self-contained.

Using the above theorem we have proved that the six commonly used 2-DOF or 3-DOF wheeled mobile robots are locally accessible. These mobile robots with different wheel and axle configurations are shown in Figure 1. The coordinates (x, y) indicate the location of the robot with respect to the world coordinate system. The angle θ gives the orientation of the vehicle or the wheels with respect to a line parallel to the x axis. In the following kinematic equations, we assume that these vehicles roll on a plane surface without slipping.

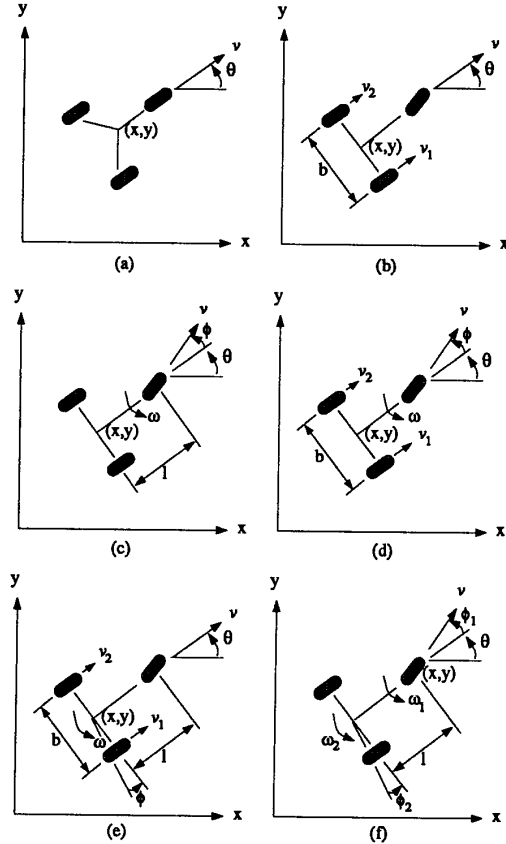


Figure 1: 2-DOF and 3-DOF Mobile Robots

Corollary 1 *The synchro-drive-and-steering-wheel vehicle (2-DOF, Equation (4), Figure 1a) is locally accessible.*

$$\dot{p} = g_1 u_1 + g_2 u_2 = \begin{bmatrix} \dot{x} \\ \dot{y} \\ \dot{\theta} \end{bmatrix} = \begin{bmatrix} \cos \theta \\ \sin \theta \\ 0 \end{bmatrix} v + \begin{bmatrix} 0 \\ 0 \\ 1 \end{bmatrix} \omega. \quad (4)$$

Corollary 2 *The two-rear-drive-wheel vehicle (2-DOF, Equation (5), Figure 1b) is locally accessible.*

$$\begin{bmatrix} \dot{x} \\ \dot{y} \\ \dot{\theta} \end{bmatrix} = \begin{bmatrix} [\cos\theta]/2 \\ [\sin\theta]/2 \\ 1/b \end{bmatrix} v_1 + \begin{bmatrix} [\cos\theta]/2 \\ [\sin\theta]/2 \\ -1/b \end{bmatrix} v_2. \quad (5)$$

Corollary 3 *The one-front-drive-and-steering-wheel vehicle (2-DOF, Equation (6), Figure 1c) is locally accessible.*

$$\begin{bmatrix} \dot{x} \\ \dot{y} \\ \dot{\theta} \\ \dot{\phi} \end{bmatrix} = \begin{bmatrix} \cos\theta\cos\phi \\ \sin\theta\cos\phi \\ [\sin\phi]/l \\ 0 \end{bmatrix} v + \begin{bmatrix} 0 \\ 0 \\ 0 \\ 1 \end{bmatrix} \omega. \quad (6)$$

Corollary 4 *The two-rear-drive-wheel and one-front-steering-wheel vehicle (3-DOF, Equation (7)², Figure 1d) is locally accessible.*

$$\begin{bmatrix} \dot{x} \\ \dot{y} \\ \dot{\theta} \\ \dot{\phi} \end{bmatrix} = \begin{bmatrix} [\cos(\theta+\phi)]/2 & [\cos(\theta+\phi)]/2 & 0 \\ [\sin(\theta+\phi)]/2 & [\sin(\theta+\phi)]/2 & 0 \\ 1/b & -1/b & 0 \\ 0 & 0 & 1 \end{bmatrix} \begin{bmatrix} v_1 \\ v_2 \\ \omega \end{bmatrix}. \quad (7)$$

Corollary 5 *The two-rear-drive-wheel and rear-steering vehicle (3-DOF, Equation (8), Figure 1e) is locally accessible.*

$$\begin{bmatrix} \dot{x} \\ \dot{y} \\ \dot{\theta} \\ \dot{\phi} \end{bmatrix} = \begin{bmatrix} [\cos\theta]/2 & [\cos\theta]/2 & 0 \\ [\sin\theta]/2 & [\sin\theta]/2 & 0 \\ 1/b + [\sin\phi]/l & -1/b - [\sin\phi]/l & 0 \\ 0 & 0 & 1 \end{bmatrix} \begin{bmatrix} v_1 \\ v_2 \\ \omega \end{bmatrix}. \quad (8)$$

Corollary 6 *The one-front-drive-and-steering-wheel and rear-steering vehicle (3-DOF, Equation (9), Figure 1f) is locally accessible.*

$$\begin{bmatrix} \dot{x} \\ \dot{y} \\ \dot{\theta} \\ \dot{\phi}_1 \\ \dot{\phi}_2 \end{bmatrix} = \begin{bmatrix} \cos(\theta+\phi_1) & 0 & 0 \\ \sin(\theta+\phi_1) & 0 & 0 \\ [\sin(\phi_1-\phi_2)]/[l\cos(\phi_1)] & 0 & 0 \\ 0 & 1 & 0 \\ 0 & 0 & 1 \end{bmatrix} \begin{bmatrix} v \\ \omega_1 \\ \omega_2 \end{bmatrix}. \quad (9)$$

For the above systems, accessibility implies controllability, as stated below.

Theorem 2 *The systems (4), (5), (6), (7), (8), and (9) are controllable.*

The above conditions and findings cover those mobile robots most commonly used in laboratories and industry. Most existing wheeled mobile robots can be characterized by the above equations or simple variations, although some mobile robots may have more than three wheels or more than one or two caster wheels. Furthermore, although the above proofs indicate that mobile robot systems are controllable, they are not stabilizable by using continuous feedback, as proved in Section 5.1.

²This and the rest of the system equations are formulated by matrix expressions to present in limited space.

It may not be true that the corresponding linearized system can be stabilized using linear feedback.

Since the above proofs have established that commonly used mobile robots are controllable, an obvious question is how to analyze and control them. We will use the synchro-drive vehicle as our prototype to demonstrate how various tools can be used to analyze a mobile robot system. We consider this system because it is commonly available and its modeling has not been discussed in the literature. We examine the vehicle kinematics, dynamics, and control in that order.

3 Kinematics of Synchro-Drive Vehicles

Forward and inverse kinematics are studied in each subsection. The determination of the degrees of freedom for synchro-drive vehicles is explained in the last subsection.

3.1 Forward Kinematics

Forward kinematics is the study of how to derive Cartesian positions and their derivatives from given input or joint variables. The center of mass motion model used for this analysis is shown in Figure 1a. As noted before, the kinematic equations of motion for the center of mass of a mobile robot in terms of its linear velocity v and angular velocity ω are

$$\dot{p} = J(p)\dot{q}, \quad (10)$$

that is,

$$\begin{bmatrix} \dot{x} \\ \dot{y} \\ \dot{\theta} \end{bmatrix} = \begin{bmatrix} \cos\theta & 0 \\ \sin\theta & 0 \\ 0 & 1 \end{bmatrix} \begin{bmatrix} v \\ \omega \end{bmatrix}, \quad (11)$$

where $0 \leq v \leq V_{max}$, $|\omega| \leq \Omega_{max}$. V_{max} and Ω_{max} are the maximum linear and angular velocities of a particular mobile robot. Integration of Equation (10) yields the vehicle positions:

$$p = \int_0^t \dot{p} d\tau = \begin{bmatrix} x_0 \\ y_0 \\ \theta_0 \end{bmatrix} + \begin{bmatrix} \int_0^t v \cos\theta d\tau \\ \int_0^t v \sin\theta d\tau \\ \int_0^t \omega d\tau \end{bmatrix}, \quad (12)$$

where x_0, y_0, θ_0 are the initial positions of the vehicle. These equations can be used to estimate the trajectories of mobile robots, as discussed in [18].

3.2 Inverse Kinematics

Inverse kinematics is the study of how to obtain the joint variables given Cartesian positions and their derivatives. A solution for \dot{q} of Equation (10) could easily be found by inverting the Jacobian matrix $J(p)$ if $J(p)$ were a square matrix. However, Equation (11) indicates that $J(p)$ is not a square matrix and that this particular system is an overdetermined system of two unknowns in three equations so that the direct inverse of the Jacobian matrix $J(q)$ is impossible. However, a least-square solution can be found by using the pseudo-inverse $[J(q)]^\dagger$ of $J(q)$ [7], as indicated below

$$\dot{q} = [J(q)]^\dagger \dot{p} = \{[J(q)]^t J(q)\}^{-1} [J(q)]^t \dot{p}, \quad (13)$$

where t denotes the transpose of a matrix and -1 denotes the inverse, that is,

$$\begin{bmatrix} v \\ \omega \end{bmatrix} = \begin{bmatrix} \cos\theta & \sin\theta & 0 \\ 0 & 0 & 1 \end{bmatrix} \begin{bmatrix} \dot{x} \\ \dot{y} \\ \dot{\theta} \end{bmatrix}. \quad (14)$$

The derivation of the above approximate solution indicates that exact continuously differentiable feedback control cannot be found by inverse kinematics. We will provide a formal proof in 5.1 to further extend this observation.

3.3 Discussion

Based on the kinematic equations derived in the previous subsection, we can decide the number of degrees of freedom for the system. From the first 2 rows of Equation (11), we can derive one independent equation of constraint in terms of the velocity

$$\dot{x}\sin\theta - \dot{y}\cos\theta = 0. \quad (15)$$

Since three coordinates (x, y, θ) are used to specify the configuration of the system and only one equation is the nonholonomic constraint equation, the synchro-drive vehicle system is clearly a 2-DOF system.

In this study, we choose a Cartesian coordinate system to represent the position of a vehicle so that the relative position of the vehicle with respect to a world coordinate system can easily be found. However, different coordinate systems can be used to describe this system. If only the local motion of the vehicle is considered, a polar coordinate system will make the analysis much simpler.

4 Dynamics of Synchro-Drive Vehicles

Inverse and forward dynamics are studied in each subsection. The general form of the dynamic equations is derived in the last subsection.

4.1 Inverse Dynamics

Inverse dynamics is the study of how to find the required torque vector from a given motion. Assume there are k rigid bodies in a synchro-drive vehicle, each with mass m_i . Because the main body of the vehicle does not rotate with respect to the world coordinate system, only l out of k bodies have moments of inertia, each with J_j . If there is no payload mounted on the spine shaft linked to the wheels, and if the moment of inertia of the gears is ignored, the only moments of inertia left are $3J_{wheel}$ for 3 wheels. Since the system cannot change its vertical position, its potential energy is a constant. Using the standard form of Lagrange's equation, we obtain the equations of motion in the matrix form

$$\begin{bmatrix} \sum_{i=1}^k m_i & 0 & 0 \\ 0 & \sum_{i=1}^k m_i & 0 \\ 0 & 0 & \sum_{j=1}^l J_j \end{bmatrix} \begin{bmatrix} \ddot{x} \\ \ddot{y} \\ \ddot{\theta} \end{bmatrix} = \begin{bmatrix} f_x + \lambda \sin\theta \\ f_y - \lambda \cos\theta \\ \tau_s \end{bmatrix}, \quad (16)$$

where λ is a Lagrange multiplier and $\sin\theta$ and $-\cos\theta$ are derived previously from constraint Equation (15). f_x and f_y are the scalar components of the external resultant force projected onto the x axis and the y axis respectively, and τ_s is the external resultant torque with respect to the vertical axis.

Let θ_s denote the steering angle of the wheel, θ_d denote the rotational angle of the wheel, and r denote the radius of the wheel. By eliminating λ and using $v = r\dot{\theta}_d$, the dynamic equations of the motion can be derived as

$$\begin{bmatrix} \sum_{i=1}^k m_i r & 0 \\ 0 & \sum_{j=1}^l J_j \end{bmatrix} \begin{bmatrix} \ddot{\theta}_d \\ \ddot{\theta}_s \end{bmatrix} = \begin{bmatrix} f_d \\ \tau_s \end{bmatrix}, \quad (17)$$

or

$$\bar{I}\ddot{\bar{p}} = \bar{\tau}. \quad (18)$$

4.2 Forward Dynamics

Forward dynamics is the study of how to characterize the motion of a mobile robot resulting from a given torque vector. By inverting Equation (17), the forward dynamic equations are obtained as

$$\begin{bmatrix} \ddot{\theta}_d \\ \ddot{\theta}_s \end{bmatrix} = \begin{bmatrix} \left(\frac{1}{\sum_{i=1}^k m_i r} \right) & 0 \\ 0 & \left(\frac{1}{\sum_{j=1}^l J_j} \right) \end{bmatrix} \begin{bmatrix} f_d \\ \tau_s \end{bmatrix}. \quad (19)$$

4.3 Discussion

This method of deriving the dynamic equations is not unique; the same result can be obtained using Newton's law and vector analysis or the Newton-Euler equation. The use of Lagrange's equation is only one method of determining the equations of motion in order to obtain the forms shown in (18). Other forms are possible.

For manipulators, the general dynamic equations can be written as

$$H(q)\ddot{q} + C(q, \dot{q})\dot{q} + G(q) = Q. \quad (20)$$

However, for mobile robots, the general dynamic equations are

$$H(p)\ddot{p} + C(p, \dot{p})\dot{p} = Q. \quad (21)$$

This form could be used for the dynamic equations of any mobile robot. At first glance, Equation (21) may look like general dynamic equations for manipulators if we add a gravitational term on the left side, but the difference is that the arguments of H and C are not unique, as in the holonomic system. The arguments could be q or p . Another difference is that Q includes a generalized constraint force, a special characteristic imposed by the nonholonomic system. Since all of the wheeled mobile robots move on planes, the gravitational is always constant. Therefore, we simply drop this term.

There are no centripetal and Coriolis accelerations relative to the center of mass, which results in the simple dynamic equations shown in Equation (18). The reason is that, because of the synchronization features, the synchro-drive robots only translate and do not rotate around the center of mass or the origin of the local coordinate system.

5 Control of Synchro-Drive Vehicles

In the first subsection, we prove the non-existence of smooth feedback control to stabilize an equilibrium point for synchro-drive vehicles. In the second subsection, we 1) examine the accessibility of synchro-drive vehicles using modified kinematic equations, 2) study the stability property of a simple controller using dynamic equations, and 3) demonstrate an important drawback of the potential-field control using an actual mobile robot system experimentally. The control of actuators with dynamics is omitted in this short paper and it can be found in [19].

5.1 Non-Existence of Continuous Control

From the discussion of inverse kinematics, we know that there is no way to find continuously differentiable feedback control for nonholonomic robot systems. This can be formally proved and extended to continuous feedback control by the theorem below.

Theorem 3 *The synchro-drive vehicle system described by Equation (4) cannot be asymptotically stabilized to a single equilibrium point by any continuous feedback control.*

Proof: The synchro-drive vehicle system can also be described by

$$\begin{cases} \dot{z}_1 = v + z_3\omega \\ \dot{z}_2 = \omega \\ \dot{z}_3 = -z_1\omega \end{cases}, \quad (22)$$

where

$$\begin{cases} z_1 = x\cos\theta + y\sin\theta \\ z_2 = \theta \\ z_3 = -x\sin\theta + y\cos\theta \end{cases}, \quad (23)$$

which is a coordinate transformation from (x, y, θ) of Equation (4). By Brockett's necessary condition 3 [5], the mapping defined from $(z_1, z_2, z_3, v, \omega)$ to $(v + z_3\omega, \omega, -z_1\omega)$ must be onto an open set containing 0 in order to make an equilibrium point asymptotically stable by any continuous differential feedback control. Assume that $(0, 0, \epsilon)$, $\epsilon \neq 0$, is an arbitrary point in the neighborhood of 0. We cannot find $(z_1, z_2, z_3, v, \omega)$ which can map to this point so this condition does not hold. Zabczyk further extended this necessary condition to continuous feedback control [17]. Therefore, the theorem holds. ■

This result indicates that a continuous feedback controller cannot be found for synchro-drive vehicles to stabilize an equilibrium point. Therefore, a discontinuous feedback controller must be applied if nonlinear control tools must be used.

5.2 Accessibility, Stability and Invariant Set

5.2.1 Accessibility with Acceleration Inputs

An interesting fact is that the synchro-drive vehicle remains accessible when the inputs are accelerations. This means that adding integrators to the control system will not change the accessibility of the system.

Corollary 7 *The synchro-drive-and-steering-wheel vehicle is locally accessible with acceleration inputs, Equation (24).*

$$\begin{bmatrix} \dot{x} \\ \dot{y} \\ \dot{\theta} \\ \dot{v} \\ \dot{\omega} \end{bmatrix} = \begin{bmatrix} v\cos\theta \\ v\sin\theta \\ \omega \\ 0 \\ 0 \end{bmatrix} + \begin{bmatrix} 0 \\ 0 \\ 0 \\ 1 \\ 0 \end{bmatrix} u_1 + \begin{bmatrix} 0 \\ 0 \\ 0 \\ 0 \\ 1 \end{bmatrix} u_2. \quad (24)$$

Comparing the above corollary with Corollary 1, we notice that the synchro-drive vehicles are accessible for both velocity and acceleration inputs. Equation (24) is the same as the "knife edge" example discussed by Bloch, McClamroch and Reyhanoglu [4]. They found a discontinuous feedback controller which stabilizes the origin for that example.

5.2.2 Stability of Point-to-Point Control

Using the dynamic equations of motion derived in subsection 4.1 and extending the work of Arimoto et al. [2] to this nonholonomic system, we can easily prove the asymptotical stability of the control laws based on feedback from mobile-robot angular positions and velocities, i.e., PD control.

Theorem 4 *Given the dynamic equations of the synchro-drive mobile robot described by*

$$\ddot{p} = \tau, \quad (25)$$

and the PD control law

$$\tau = -K_p \dot{p}_e - K_d \ddot{p}_e, \quad (26)$$

where $p_e = p - p_d$, p_d is a fixed vector of the desired angular position, and K_p and K_d are symmetric positive-definite constant matrices, the equilibrium point p_d , $\dot{p} = 0$ is globally asymptotically stable.

This theorem is only for the stability of a stationary desired angular position using a simple PD controller. It demonstrates why mobile robots function under simple control. We point out, however, that the above stability property provides little or no information regarding the detailed performance of our complex nonlinear synchro-drive-vehicle system.

5.2.3 Invariant Set of Potential-Field Control

After a theoretical study of the analysis of linear and nonlinear control techniques, we consider an important aspect of the popular potential-field control method which is difficult to analyze mathematically. This control method uses the vectorial sum of the virtual repulsive forces and the virtual attractive force to provide a resultant force to guide the vehicle, as shown in Figure 2. Again we use the synchro-drive vehicle as our analysis model. Since the majority of users are interested in the trajectories generated by various control methods, we consider only the effect of the potential-field method on the trajectories. In the following discussion, s denotes the position of the robot and is a function of time.

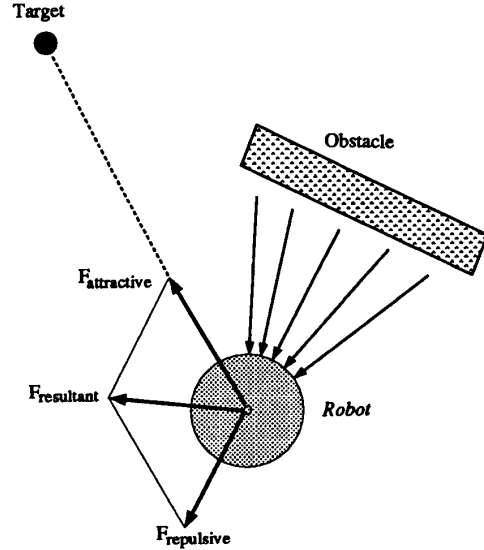


Figure 2: Potential-Field Control

Definition 1 A set $S_{\text{invariant}} \in S \subset R^n$ is said to be an invariant set of a particular mobile robot system if every trajectory of the system that starts from an initial position $s_0 \in S_{\text{invariant}}$ stays within $S_{\text{invariant}}$ at all future times.

The existence of an invariant set was verified under potential-field control with our experimental robot, a modified Cybermation K2A robot. However, this existence is difficult to prove analytically. The experimental result is shown in Figure 3.

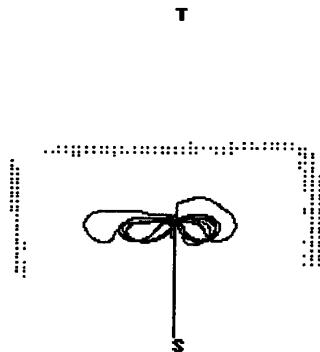


Figure 3: An Invariant Set under Potential-Field Control

In this figure, the obstacles detected by ultrasonic sensors are represented by the collections of small dots. The starting position and the target position are represented by 'S' and 'T', respectively. The robot trajectories are depicted by the continuous "figure eight" curve. This result indicates convergence to a stable limit cycle in which the mobile robot was trapped, although the underlying position-control systems are stable, as shown in [19].

6 Conclusions

A differential geometry approach was used to prove that commonly used mobile robots are controllable. Then we provided a general form for the dynamic description of mobile robots in conjunction with a systematic study of the synchro-drive vehicle. We proved that continuous feedback stabilization to an equilibrium point is impossible. We demonstrated that a simple PD controller at the second lowest level would produce a stable mobile robot system and indicated that popular potential-field methods could lead the trajectories of the robot to an invariant set and associated limit cycle performance. This study should provide a useful framework for those interested in the design, modeling, and control of mobile robots. Although most analyses of kinematics, dynamics and control are based on the synchro-drive vehicle, our general approach can easily be applied to any mobile robot system.

Limit cycle performance is a major problem in potential-field navigation. We have developed and tested a navigation algorithm to overcome this problem. A detailed experimental and theoretical evaluation of this algorithm is described in [18].

Acknowledgements

We wish to acknowledge the discussions and comments provided by Professor Michael W. Walker, Mr. Mahmut Reyhanoglu and Ms. Ming Xiang.

References

- [1] J. C. Alexander and J. H. Maddocks, "On the Kinematics of Wheeled Mobile Robots", *Int. J. Robotics Research*, vol. 8, no. 5, pp. 15-27, Aug. 1989.
- [2] S. Arimoto and F. Miyazaki, "Stability and Robustness of PID Feedback Control for Robot Manipulators of Sensory Capability", *Robotics Research: The First Int. Symp.*, M. Brady and R. P. Paul (Eds.), Cambridge, MA: MIT Press, 1984, pp. 783-799.
- [3] J. Barraquand and J. C. Latombe, "Nonholonomic Multi-body Mobile Robots: Controllability and Motion Planning in the Presence of Obstacles", *Proc. IEEE Int. Conf. Robotics and Automation*, pp. 2328-2335, Apr. 1991.
- [4] A. M. Bloch, N. H. McClamroch, and M. Reyhanoglu, "Controllability and Stabilizability Properties of a Non-holonomic Control Systems", *Proc. IEEE Conf. Decision and Control*, pp. 1312-1314, Dec. 1990.
- [5] R. W. Brockett, "Asymptotic Stability and Feedback Stabilization", *Differential Geometric Control Theory* R. W. Brockett, R. S. Millman and H. J. Sussmann (Eds.), Birkhäuser: Birkhäuser Boston, Inc., 1983.
- [6] B. d'Andréa-Novell, G. Bastin, and G. Campion, "Modelling and Control of Nonholonomic Wheeled Mobile Robots", *Proc. IEEE Int. Conf. Robotics and Automation*, pp. 1130-1135, Apr. 1991.
- [7] G. H. Golub and C. F. Van Loan, *Matrix Computations*, Baltimore, Maryland: Johns Hopkins University Press, 1983.
- [8] D. T. Greenwood, *Principles of Dynamics*, Second Edition, Englewood Cliffs, New Jersey: Prentice-Hall, Inc., 1988.
- [9] J. M. Holland, "Rethinking Robot Mobility", *Robotics Age*, vol. 7, no. 1, pp. 26-30, Jan. 1985.
- [10] A. Isidori, *Nonlinear Control Systems: An Introduction*, Second Edition, Berlin: Springer-Verlag, 1989.
- [11] G. Lafferriere and H. Sussmann, "Motion Planning for Controllable Systems Without Drift", *Proc. IEEE Int. Conf. Robotics and Automation*, pp. 1148-1153, Apr. 1991.
- [12] Z. Li and J. Canny, "Motion of Two Rigid Bodies with Rolling Constraint", *IEEE Trans. Robotics and Automation*, vol. 6 no. 1, pp. 62-72, Feb. 1990.
- [13] P. F. Muir, "Modeling and Control of Wheeled Mobile Robots", *Ph.D. Thesis, Carnegie Mellon University*, Aug. 1988.
- [14] H. Nijmeijer and A. J. van der Schaft, *Nonlinear Dynamical Control Systems*, New York: Springer-Verlag, 1989.
- [15] S. K. Saha and J. Angeles, "Kinematics and Dynamics of a Three-Wheeled 2-DOF AGV", *Proc. IEEE Int. Conf. Robotics and Automation*, pp. 1572-1577, May 1989.
- [16] E. Wilson, "Denning Mobile Robotics: Robots Guard Pen", *High Technology*, vol. 5, no. 6, pp. 15-16, June 1985.
- [17] J. Zabczyk, "Some Comments on Stabilizability", *Applied Mathematics and Optimization*, vol. 19, no. 1, pp. 1-9, Jan. 1989.
- [18] Y. Zhao and S. L. BeMent, "Experimental and Mathematical Studies of Obstacle Avoidance in Mobile-Robot Navigation thru Unknown Environments", *Robot Systems Division, CRIM, The University of Michigan*, Tech. Rep. RSD-TR-1-91, June 1991.
- [19] Y. Zhao, "Theoretical and Experimental Studies of Mobile-Robot Navigation", *Ph.D. Thesis, The University of Michigan*, 1991.